ACTIVE DISTURBANCE REJECTION CONTROL WITH DECOUPLING CASE FOR A LOWER LIMB EXOSKELETON OF SWING LEG

Nasir Ahmed Alawad[1], Amjad Jaleel Humaidi[2]
and Ahmed Sabah Alaraji[3]

[1]Department of Computer Engineering
Faculty of Engineering
Mustansiriyah University
Palestine Street, Al-Waziriyah, Baghdad 10052, Iraq
nasir.awad@uomustansiriyah.edu.iq

[2]Department of Control and System Engineering
[3]Department of Computer Engineering
University of Technology
Al-Sina'a Street, Baghdad 10066, Iraq
{ amjad.j.humaidi; ahmed.s.alaraji }@uotechnology.edu.iq

Abstract. *In this research, a decoupling active disturbance rejection control (DADRC) is developed to deal with the uncertainties and unknown disturbance in order to improve the control of the direct-driven exoskeleton. The exoskeleton's dynamic model during the swing phase was built. The swing leg's exoskeleton was then provided of a DADRC. Dynamic decoupler used in this work depends on physical model elements of exoskeleton and controller parameters. The simulations were performed with comparisons to the coupling active disturbance rejection control (CADRC) in order to validate the effectiveness of the suggested control strategy. The results revealed that the DADRC is superior to CADRC with a higher response and lower tracking error to the desired value, as well as the ability to alleviate some chattering phenomena with less torque. Root mean square error is used as a performance index for comparison purpose. The DADRC approach reduces the tracking error by more than 92.8% for the hip and 86.9% for the knee when compared to the CADRC method. The rehabilitation system can follow the desired gait more precisely with the suggested DADRC. In this research, MATLAB and SIMULINK are used to simulate the controlled system.*
Keywords: Lower-limb assistance, Exoskeleton, Decouple controller, ADRC, Human gait tracking

1. **Introduction.** Exoskeleton research is currently receiving a lot of attention because of its potential to improve human performance and aid in the recovery of some patients. Exoskeletons for the lower limbs, upper limbs, and the entire body have all been developed during the past few decades thanks to advancements in robotics and mechatronics technology. The lower limb exoskeleton, which has many mechanical structure types, actuators, and control techniques, has drawn significant attention from several institutes throughout the world [1].

The exoskeleton design involves attaching the entire limb to the rehabilitation device and controlling the limb to carry out intricate rehabilitation exercises locally or entirely [2,3]. Despite significant advancements made over decades of development, the exoskeleton's control strategy still poses a significant barrier to its widespread use. Numerous

solutions have been put up to address the exoskeleton system's excessive coupling, nonlinearity, and randomness. Exoskeletons that boost load-carrying capacity are often handled using a sensitivity amplification control, and this type of methods heavily relies on the nonlinear dynamic model [4].

Various control strategies have been established for the advancement of lower limb robotic rehabilitation exoskeletons (LLRRE) for human assistance. In the absence of disturbance, proportional-derivative (PD) based control performs well [5], but typically suffers when the disturbance occurs in the system [6]. In [7], the active force rejection control based on particle swarm optimization (PSO) is introduced as a method for rejecting disturbances in gait trajectory tracking, which necessitates the evaluation of numerous parameters. Depending on how precisely the system is modeled, computed-torque control (CTC) [8,9] may need additional control to account for modeling flaws. Innovative command rules formulation and inference testing in techniques [10] demand a lot of work. Radial basis functions (RBF) neural networks are used to correct for the disturbance but have high computational costs. Sensitivity amplified suffers from the introduction of disturbance and requires an appropriate inverse dynamic model [11,12].

One solution in these situations is robust control techniques, although these methods are conservative and take the worst-case possibilities into account at the expense of giving up the transient response [13]. Although the sliding mode control (SMC) technique can regulate parameter variations and uncertainty, it has chattering issues because of discontinuous switching [14]. To get over these contemporary control problems, active disturbance rejection control, also known as feedback linearization because it is designed on the basis of the linearization model. Han offered the ADRC as a way to eliminate disturbances, and because of its higher functionality and usefulness, it was predicted to displace the PID method [15].

Multiple controllers have been used to implement ADRC, including fuzzy control to enhance quick tracking [16], sliding mode control to provide robustness [17], and traditional PID control [18]. Additionally, the SCARA robot uses the ADRC to track a predetermined route [19]. All of these uses highlight the benefits of the ADRC in estimating external disturbances. To the authors' knowledge, however, reports about the use of the ADRC in the lower limb exoskeleton are rare.

Its popularity in motion control [20], flight control [21], and process control [22] applications, as well as in many other fields [23], is demonstrated by the evolution and rapid use of ADRC in industries over the past three decades. The architecture of ADRC is created to achieve the best performance by actively eliminating the internal and external uncertainties as a whole disturbance [24]. It is designed on error-driven control scheme [15] as opposed to model-based control law and does not require full knowledge of the model or system dynamics, i.e., it does not require an exact model of the system [25]. The ADRC is a model-free controller that just needs to know the system order and an approximation of the value of the system parameters [26].

Due to its ubiquity and efficiency, ADRC has recently been applied to numerous robotic rehabilitation devices for tracking purposes. In [27], where clinical gait data is employed as a reference, a linear extended state observer (LESO) based ADRC has been used to the lower limb exoskeleton for the hip and knee joints. When PID and ADRC results are compared for the hip and knee trajectories based on error comparison, the results indicate that ADRC performs better than PID. The lower-limb rehabilitation device, however, cannot directly train a specific region of the limb; instead, it typically has a training effect on the entire limb. In order to better understand how to increase the relevance and effectiveness of training, the exoskeleton rehabilitation device has emerged as a new research focus in the field of rehabilitation devices [28].

In summary, the majority of the existing rehabilitation equipment is centered on the mechanical structure's optimization, and the designer neglects to consider the user's needs,

particularly those of old or disabled users. In this study, we introduce an assistive lower-limb exoskeleton and apply a decoupling control technique to providing stability control. This is based on the understanding of the art and integrated with the user experience. To confirm its viability in terms of the suggested design and control approach, simulation and a human interaction test were performed. The following are the article's primary contributions.

1) To assess the needs of elderly or disabled users for rehabilitation training as closely as possible, an active assistive lower-limb exoskeleton is explored in light of user experience.

2) To achieve the high safety requirements for the rehabilitation training, the decoupler approximation-based position tracking controller is used.

3) The comparison tracking performance using the proposed DADRC method and the CADRC method is shown, demonstrating that the elderly can be served by the produced rehabilitation device.

The modeling of suggested exoskeleton system is provided in Section 2. The analysis of ADRC approach has been presented in Section 3. In Section 4, the Decoupling Control Structure Based on ADRC for Exoskeleton system has been analyzed. Section 5 conducted numerical simulation and discussion of simulated results. Section 6 has drawn the conclusions of this study based on simulated results.

2. **Lower Limb Rehabilitation Exoskeleton Modeling.** The link between the motion of the hip and knee joints and the control torque can be calculated using the dynamic model of the lower limb rehabilitation exoskeleton. A simplified structure diagram of the lower limb was developed in the sagittal plane, as seen in Figure 1, ignoring the impact of ambient interference on the lower limb rehabilitation exoskeleton, we examine a 2-degree of freedom (DOF) of lower limb rehabilitation exoskeleton. Anthropometric information for a person weighing 74 kg and standing 1.69 m tall was published by [29], and this information was used by [30] to create the dynamic model of this robot. A second-order nonlinear differential equation can be utilized to define the dynamic model of the lower limb rehabilitation exoskeleton robot, which is established using the Lagrange approach [30,31].

$$M(\theta)\ddot{\theta}(t) + C\left(\theta, \dot{\theta}\right)\dot{\theta}(t) + G(\theta) + d(t) = u(t) \tag{1}$$
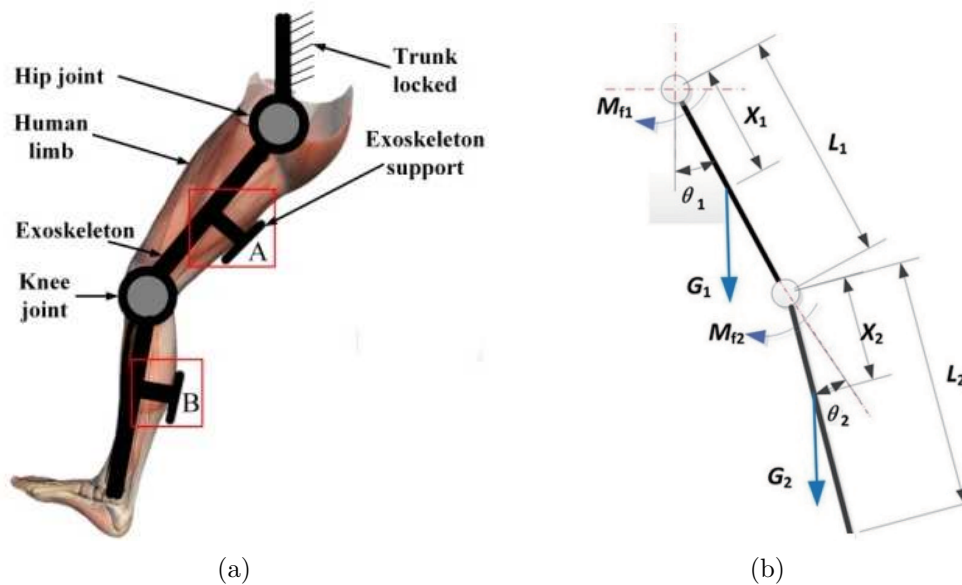

FIGURE 1. (a) Physical prototype of the exoskeleton; (b) the schematic diagram of a wearable exoskeleton

or, in matrix form as:

$$
\begin{bmatrix} M_{11} & M_{12} \\ M_{21} & M_{22} \end{bmatrix} \begin{bmatrix} \ddot{\theta}_1 \\ \ddot{\theta}_2 \end{bmatrix} + \begin{bmatrix} C_{11} & C_{12} \\ C_{21} & C_{22} \end{bmatrix} \begin{bmatrix} \dot{\theta}_1 \\ \dot{\theta}_2 \end{bmatrix} + \begin{bmatrix} d_1(t) \\ d_2(t) \end{bmatrix} + \begin{bmatrix} G_1(\theta) \\ G_2(\theta) \end{bmatrix} = \begin{bmatrix} u_1(t) \\ u_2(t) \end{bmatrix} \quad (2)
$$

where θ, $\dot{\theta}$, and $\ddot{\theta}$ respectively represent the angle, angular velocity, and acceleration of a robot joint vector. $M(\theta) \in R^{(2*2)}$ are matrices of human limbs for each inertia. Coriolis and centrifugal torque are given by $C\left(\theta, \dot{\theta}\right) \in R^{(2*2)}$. The torque of gravity $(G(\theta))$ has one-dimensional vector $\in R^{(2*1)}$. $d(t) \in R^{(2*1)}$ is the vector of external disturbance, and $u(t) \in R^{(2*1)}$ indicates the control signal [30]. The inertial matrix $M(\theta)$ can be represented as below.

$$
\begin{aligned}
M_{11}(\theta) &= I_1 + I_2 + M_{f1}(x_1)^2 + M_{f2}(L_1)^2 + M_{f2}(x_2)^2 + 2M_{f2}x_1x_2\cos(\theta_2) \\
M_{12}(\theta) &= M_{21}(\theta) = I_2 + M_{f2}(x_2)^2 + M_{f2}L_1x_2\cos(\theta_2) \\
M_{22}(\theta) &= I_2 + M_{f2}(x_2)^2
\end{aligned} \quad (3)
$$

The Coriolis and centrifugal force matrix $C(\theta)$ can be represented as the following:

$$
\begin{aligned}
C_{11} &= -M_{f2}L_1x_2\sin(\theta_2)\dot{\theta}_2 \\
C_{12} &= -M_{f2}L_1x_2\sin(\theta_2)\left(\dot{\theta}_1 + \dot{\theta}_2\right) \\
C_{21} &= M_{f2}L_1x_2\sin(\theta_2)\dot{\theta}_1 \\
C_{22} &= 0
\end{aligned} \quad (4)
$$

The gravitational item $G(\theta)$ can be represented as

$$
\begin{aligned}
G_1 &= M_{f1}x_1g\sin(\theta_1) + M_{f2}gL_1\sin(\theta_1) + M_{f2}gx_2\sin(\theta_1 + \theta_2) \\
G_2 &= M_{f2}gx_2\cos(\theta_1 + \theta_2)
\end{aligned} \quad (5)
$$

The physical parameters of the simplified structure are shown in Table 1.

TABLE 1. The variables definition for LLRRE [30]

Parameters	Definitions	Units	Values
L_1	Hip length	m	0.54
L_2	Knee length	m	0.48
x_1	Center of hip mass	m	0.2338
x_2	Center of knee mass	m	0.241
M_{f1}	Hip mass	Kg	8
M_{f2}	Knee mass	Kg	3.72
I_1	Hip inertia	Kg·m^2	0.42
I_2	Knee inertia	Kg·m^2	0.07
g	Gravity	m/s^2	9.8
θ_{1d}	Angular displacement of hip	Rad	–
θ_{2d}	Angular displacement of knee	Rad	–
$\dot{\theta}_1$	Angular velocity of hip	Rad/s	–
$\dot{\theta}_2$	Angular velocity of knee	Rad/s	–
$\ddot{\theta}$	Angular acceleration	Rad/s^2	–

3. **General Form of ADRC.** The extended state observer (ESO), which can estimate dynamic uncertainty and applied torques without the need for a comprehensive system model, is the core of ADRC. In order to approximately capture the overall system uncertainties and external disruptions in real time, this efficient approach extends another state. It is possible to formulate Equation (1) for a second-order nonlinear system as follows [32-34]:

$$\ddot{\theta} = f\left(t, \theta, \dot{\theta}, \omega\right) + b_o T \tag{6}$$

or in state-space form:

$$\begin{aligned}
\dot{x}_1 &= x_2 \\
\dot{x}_2 &= x_3 + b_o T \\
\dot{x}_3 &= \dot{f} \\
y &= x_1
\end{aligned} \tag{7}$$

where θ is the desired trajectory signal that must be controlled, b_o is a boundary that is generally known, and T is the required torque. The term f addresses the joined impact of the inner elements and external disturbances ω. An extended state observer (ESO) is utilized for this, which permits an approximate estimate task to be performed with adequate accuracy for the algorithms functioning. When an ESO is used to estimate f and it corresponds to the system $(x_1, x_2, \ldots, x_n, x_{n+1})$, there will be an accurate estimate of $(y, \dot{y}, \ldots, y^{n-1}, f)$. The observer of Equation (7), in this case takes the form of the most widely used linear Luenberger-like estimator, which is [35-37]

$$\begin{aligned}
\dot{z} &= A\tilde{z} + \tilde{b}T + L\left(z - \tilde{z}\right) \\
\tilde{y} &= C\tilde{z}
\end{aligned} \tag{8}$$

where $\tilde{z} = [\widetilde{z_1} \quad \widetilde{z_2} \quad \widetilde{z_3}]^T$ are the vectors of estimates of y, $\dot{y}$, and f, respectively. When properly designed and implemented, the state of the observer equation (8) will track that of the plant equation (6). The parameter vector L can be obtained using, for example, the pole-placement method [38]. For the simplicity, let the characteristics equation for ESO design be

$$Q(s) = |SI - (A - LC)| = (S + W_o)^3 \tag{9}$$

where S denotes Laplace-operator, I is a unity matrix, A is the system matrix, C is the output vector, and L is the vector of observer gains. The observer bandwidth can be used to calculate the observer gains as follows

$$L = \left[\begin{array}{ccc} 3W_o & 3W_o^2 & W_o^3 \end{array}\right]$$

When estimate $\widetilde{z_3}$ and approximately equal to the total disturbance f, the following control law can be obtained [15]:

$$T = \frac{(U_o - f)}{b_o} \tag{10}$$

So Equation (6) can be reduced to an approximate double integral plant: $\ddot{\theta} = U_o$, and in this case can be easily controlled using a PD controller of the form:

$$U_o = k_p\left(\theta_d - \widetilde{z_1}\right) + k_d\left(\dot{\theta}_d - \widetilde{z_2}\right) \tag{11}$$

where U_o is the output of the PD controller. Plainly, the critical thought in ADRC is to appraise f continuously and drop it in the regulator law. For regulator tuning to calculate k_p and k_d, these qualities rely upon controller bandwidth W_c as

$$\begin{aligned}
k_p &= W_c^2 \\
k_d &= 2W_c
\end{aligned} \tag{12}$$

This is related to design specifications, specially the settling time T_s, so that [39]

$$W_c = \frac{10}{T_s} \tag{13}$$

In this study, if selecting $T_s = 0.4$ sec, then $W_c = 24.5$ rad/sec and the value (W_o) is calculated as

$$W_o = 4W_c$$

Equation (6) can be repeated for hip and knee and design ADRC for each loop, as shown in the next section.

4. **Decoupling Control Structure Based on ADRC for Exoskeleton.** The exoskeleton leg dynamics model in this study is a multi-input, multi-output (MIMO) system, depending on the robotic exoskeleton dynamics model represented by Equation (1). The following is an expression for the mathematical model of a robotic exoskeleton:

$$M_{11}\ddot{\theta}_1 + M_{12}\ddot{\theta}_2 + C_{11}\dot{\theta}_1 + C_{12}\dot{\theta}_2 + G_1 + D_1 = T_1$$
$$M_{21}\ddot{\theta}_1 + M_{22}\ddot{\theta}_2 + C_{21}\dot{\theta}_1 + C_{22}\dot{\theta}_2 + G_2 + D_2 = T_2 \tag{14}$$

where (T_1, T_2), (θ_1, θ_2) represent torques required and desired position trajectory for hip, and knee, respectively. Equation (14) is programmed and needs two loops of ADRC in order to verify the effectiveness of the proposed robust ADRC control with decoupling effect between these loops.

And $D = [D_1 \quad D_2]^T$ and $T = [T_1 \quad T_2]^T$, D_1 and D_2 are external disturbances and un-modeled dynamics, T_1 and T_2 are the input torques of the hip joint and the knee joint. The next step is to transfer (14) to the state space expression:

$$\ddot{\theta}_1 = \frac{1}{M_{11}M_{22} - M_{21}M_{12}}(M_{22}T_1 - M_{12}T_2 - H_1)$$
$$\ddot{\theta}_2 = \frac{1}{M_{11}M_{22} - M_{21}M_{12}}(M_{21}T_1 - M_{11}T_2 - H_2) \tag{15}$$

where

$$H_1 = (M_{22}C_{11} - M_{12}C_{21})\dot{\theta}_1 + (M_{22}C_{12} - M_{12}C_{22})\dot{\theta}_2 + M_{22}G_1 - M_{12}G_2$$
$$\qquad + M_{22}D_1 - M_{12}D_2$$
$$H_2 = (-M_{21}C_{11} - M_{11}C_{21})\dot{\theta}_1 - (M_{21}C_{12} - M_{11}C_{22})\dot{\theta}_2 - M_{21}G_1 + M_{11}G_2$$
$$\qquad - M_{22}D_1 + M_{12}D_2 \tag{16}$$

Equation (15) can be rewritten as

$$\ddot{\theta}_1 = V_1(M_{22}T_1 - M_{12}T_2) + h_1$$
$$\ddot{\theta}_2 = -V_1(M_{21}T_1 - M_{11}T_2) + h_2 \tag{17}$$

where

$$V_1 = \frac{1}{M_{11}M_{22} - M_{21}M_{12}}, \quad h_1 = -H_1V_1, \quad h_2 = -H_2V_1 \tag{18}$$

The system in Equation (17) is decoupled by matrix D_e.

$$D_e = \begin{pmatrix} V_1M_{22} & 0 \\ 0 & V_1M_{11} \end{pmatrix} \tag{19}$$

So, the ADRC control law (U) for standard second order system (hip or knee) can be expressed as

$$U = [(k_p e + k_d \dot{e} + \widetilde{z}_3) - f]/b_o$$

And according to this law, the required torque for each loop is

$$T = [T_1 \quad T_2]^T = D_e^{-1} * U = D_e^{-1}(k_p e + k_d \dot{e} - \widetilde{z}_3)/b_o \tag{20}$$

when $\widetilde{z}_3 = f$.

Figure 2 shows decoupling control structure based on ADRC. θ_{1d} and θ_{2d} are desired hip and knee trajectories, respectively. TD is tracking differentiator, which gives the same desired input signal and its derivatives.
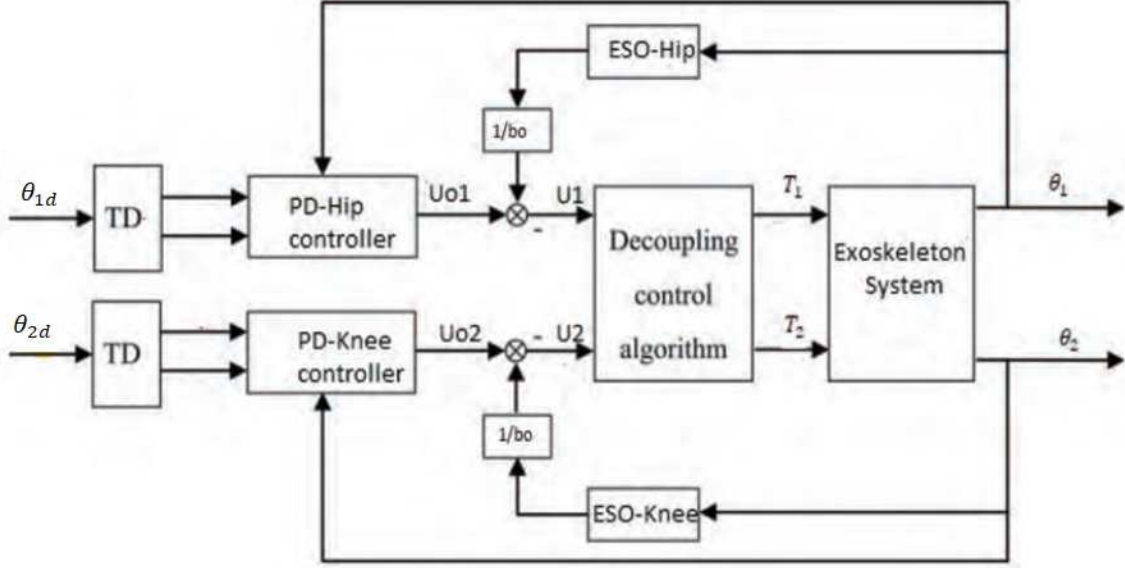

FIGURE 2. Decoupling control structure based on ADRC

Return to Equation (20), and assume that the control design objective is to make the output of the plant follow a given, bounded, reference signal θ_{id}, whose derivatives, $\dot{\theta}_{id}, \ddot{\theta}_{id}, \ldots, \theta_{id}^{(n)}$, are also bounded. To study the stability for each joint (hip and knee). Let us firstly consider the hip joint

$$e_i = \theta_{1d} - z_i, \text{ for } i = 1, 2, \ldots, n \text{ and } \dot{e} = A_e e + A_q \tilde{z}, \text{ where}$$

$$A_e = \begin{bmatrix} 0 & 1 \\ -k_{p,1} & -k_{d,1} \end{bmatrix}, \quad A_q = \begin{bmatrix} 0 & 0 & 0 \\ 0 & 0 & 0 \\ -k_{p,1} & -k_{d,1} & -1 \end{bmatrix}, \quad \tilde{z} = \begin{bmatrix} \widetilde{z_1} \\ \widetilde{z_2} \\ \widetilde{z_3} \end{bmatrix} \quad (21)$$

where $k_{p,1}$, $k_{d,1}$ are proportional and derivative controller gains, respectively. Similarly, for the knee joint, repeat Equation (21), since all gains of (k_p, k_d) for hip and knee are selected in such a way that, $s^2 + k_d s + k_p$ is Hurwitz, and A_e is Hurwitz. For tuning simplicity we just let [40]

$$s^2 + k_d s + k_p = (s + W_c)^2 \quad (22)$$

where $W_c > 0$. This makes W_c the only tuning parameter such that

$$\lim_{n \to \infty} e_i(t) = 0, \text{ for } i = 1, 2, \ldots, n$$

From the above, it is shown that the closed loop system is asymptotically stable. The same conclusion can be reached for knee joint.

5. **Result Analysis and Discussion.** On the basis of previous work, the MATLAB/Simulink simulation of the DADRC for LLRRE was performed in this section, and the CADRC controller was also used for comparison. The desired hip and knee joint trajectories are established by the clinical gait analysis (CGA). You can utilize the fitting functions listed below:

$$\theta_{1d} = 1.2 \sin\left(\frac{pi}{2}t\right)$$

$$\theta_{2d} = -1.2 \sin\left(2\frac{pi}{3}t\right)$$

where t is the time interval, which can be anywhere between 0 and 8 seconds. The same gains for hip and knee ($k_p = 600$, $k_d = 49$), also the observer gains ($L_1 = 288$, $L_2 = 28812$, $L_3 = 94119$) are taken for CADRC and DADRC. The root mean square error (RMSE) is used as the performance index for comparison while recording each performance [32,41]. The tracking results for the two controllers are displayed in Figures 3 and 4. All of the data clearly demonstrate that these techniques can follow the desired trajectory to the LLRRE system at a macro level. However, it is evident that DADRC performs better than CADRC, particularly at the beginning of work. Additionally, there is no chattering as a result of DADRC's decoupler algorithm effect, and this is seen in both hip and knee loops. From Figure 3, it is easy to find that the DADRC is able to track with the desired input and rapid response at the beginning of 0.15 s, when compared with CADRC at 0.2 sec.
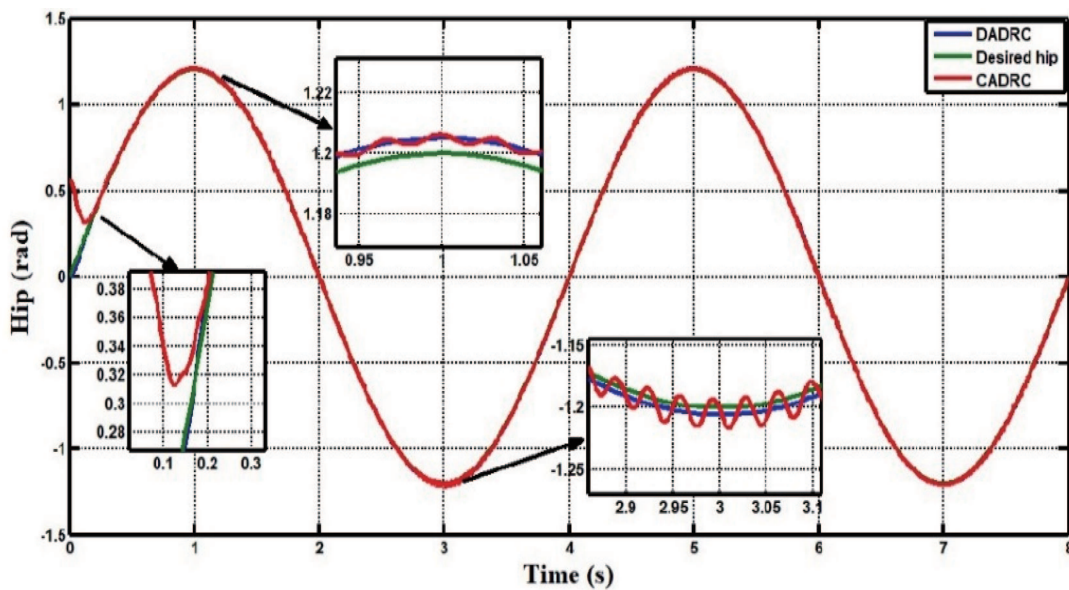

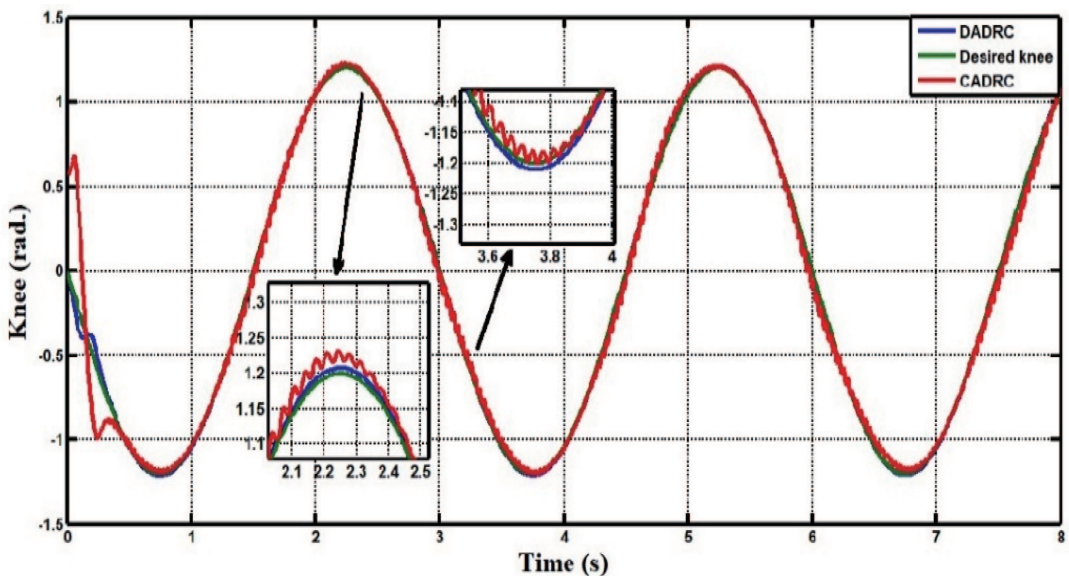FIGURE 3. (color online) The results of simulations for hip tracking performance

FIGURE 4. (color online) The results of simulations for knee tracking performance

In contrast to CADRC, which performs marginally worse with chattering as demonstrated in Figure 5 for hip trajectory, DADRC is better able to follow the ideal trajectory of human joints with less error. The similar analysis may be applied to the knee trajectory depicted in Figure 6, but with higher inaccuracy because the knee's initial starting point is more divergent and noisy than the desired trajectory. Compared to CADRC, the RMSE for DADRC to the hip joints are 0.0051 rad and 0.0712 rad for CADRC. The knee position trajectory for DADRC is more accurate than CADRC, as evidenced by the RMSE values of 0.016 rad and 0.1234 rad for CADRC.
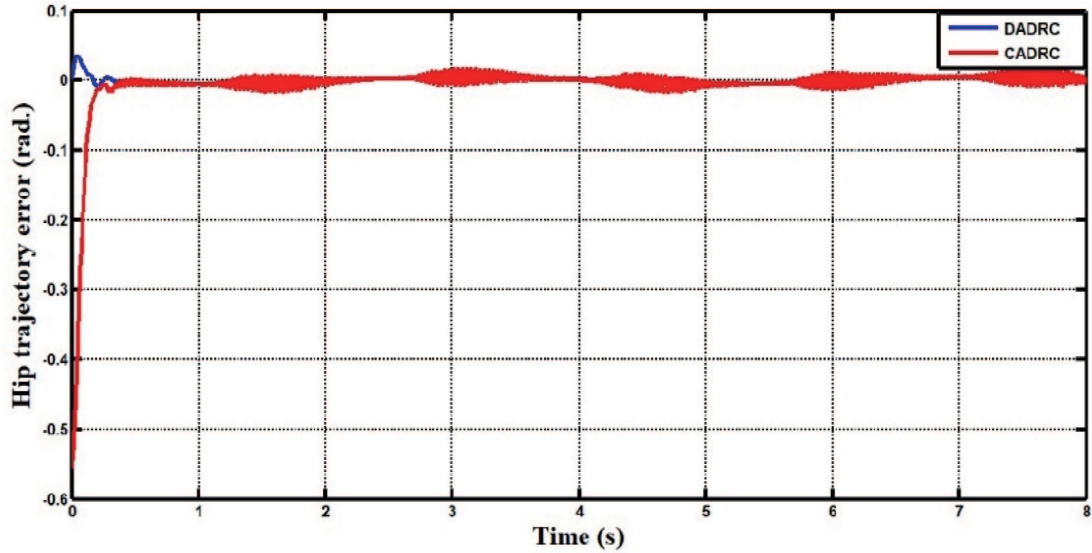

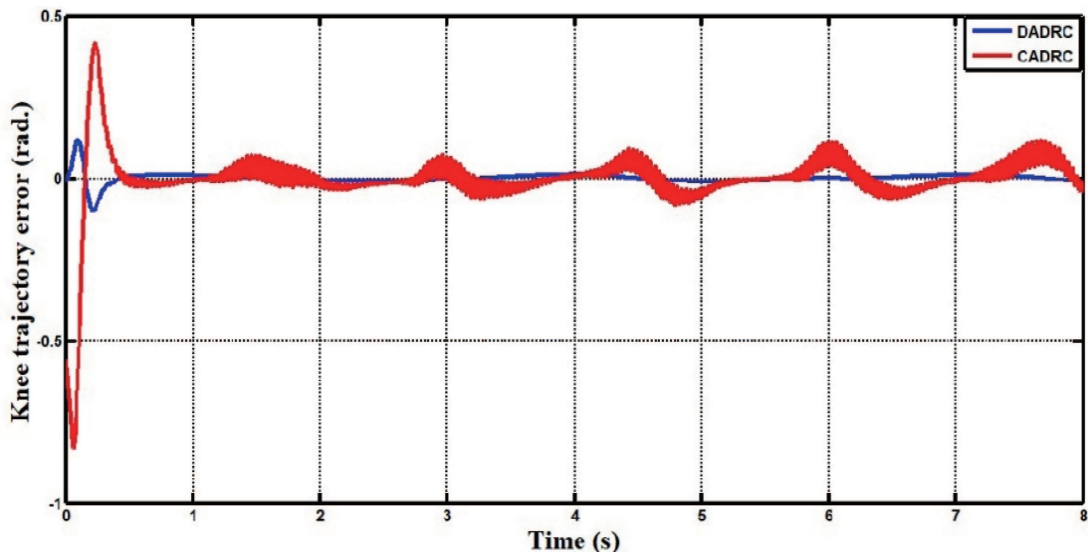FIGURE 5. (color online) The errors of the two controllers for hip trajectory

FIGURE 6. (color online) The errors of the two controllers for knee trajectory

The torques of hip and knee are presented in Figures 7 and 8. The driving torques are large at the beginning in both of the joints. However, the max torque of two joints using DADRC is the smallest at steady-state without chattering, while the outcomes of CADRC are the biggest with more chattering due to the coupling effect between the two joints. In general, the required hip torque is more than knee due to the starting moving at the hip joint, so it needs more torque.
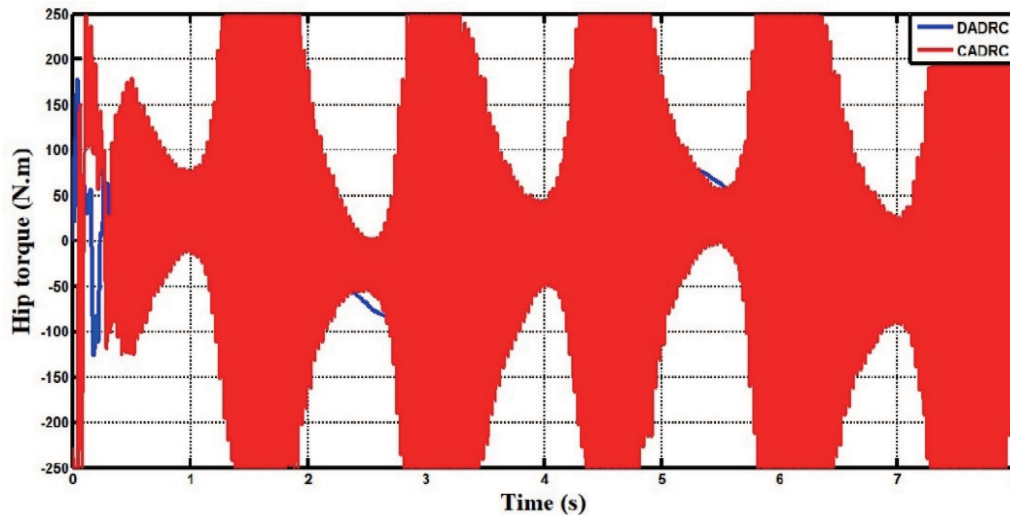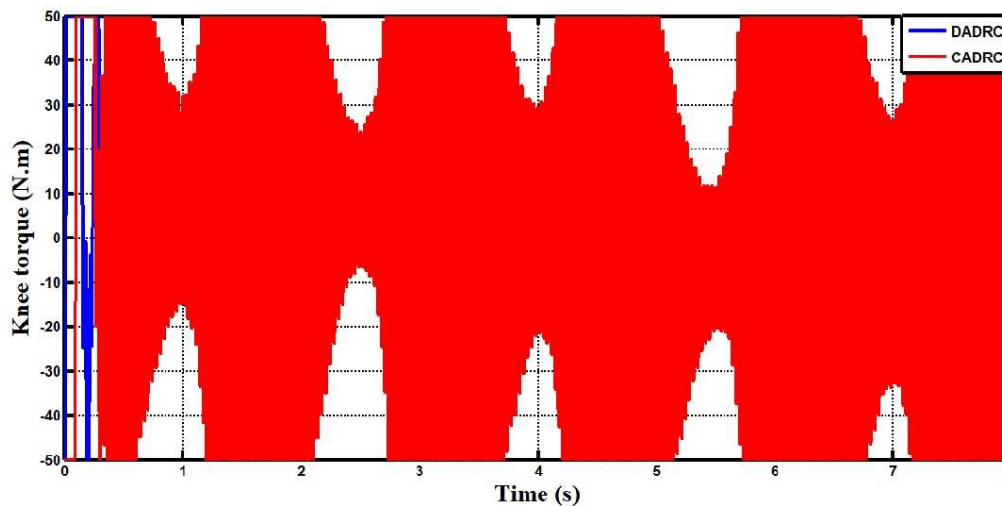
FIGURE 7. (color online) The driving torque of hip

FIGURE 8. (color online) The driving torque of knee

6. **Conclusion.** This paper presented a DADRC to control the LLRRE for a swing leg tracking with the trajectories of human hip and knee joints. The simulation was successfully completed with the application of this control strategy, and when compared to the CADRC, the results demonstrate that the DADRC is capable of leading the leg of the LLRRE to swing like a human, with strong anti-jamming capabilities, high tracking performance, and a lower requirement for maximum driving torque in this work. As a result, the current approach can be used to control LLRRE in swing phase and reject the disturbance. When compared to the conventional position control approach, the DADRC has the ability to perform admirably throughout the early stages of rehabilitation. It can also be applied to various rehabilitation exoskeletons control. The target trajectory is tracked using the proposed control method (DADRC), which proved that it is both faster and more accurate than the CADRC for both joints. DADRC requires less power to start moving the D.C. motor (175 N·m for the hip and 50 N·m for the knee) than CADRC, which requires ±250 N·m for the hip and ±50 N·m of variable torque (chattering) throughout the entire task for eight seconds.

The DADRC will eventually be developed and expanded to a physical exoskeleton prototype for additional validation and practical use of the suggested technique in future. To conduct a comparison research for this medicinal application, alternative control strategies could be recommended [42-50].

REFERENCES

[1] Y. X. Ma, J. Yi, C. Wang and C. Chen, A review on human-exoskeleton coordination towards lower limb robotic exoskeleton systems, *Int. J. Robot. Autom.*, vol.34, no.4, pp.431-451, 2019.

[2] A. Gupta and M. K. O'Malley, Design of a haptic arm exoskeleton for training and rehabilitation, *IEEE/ASME Trans. Mechatron.*, vol.11, no.3, pp.280-289, DOI: 10.1109/TMECH.2006.875558, 2006.

[3] B. Chen, H. Ma, L. Y. Qin, F. Gao, K. M. Chan, S. W. Law, L. Qin and W. H. Liao, Recent developments and challenges of lower extremity exoskeletons, *J. Orthop. Transl.*, vol.5, pp.26-37, 2016.

[4] R. Baud, A. R. Manzoori, A. Ijspeert et al., Review of control strategies for lower-limb exoskeletons to assist gait, *Journal of NeuroEngineering and Rehabilitation*, vol.18, Article no. 119, DOI: 10.1186/s12984-021-00906-3, 2021.

[5] J. L. Emken, S. J. Harkema, J. A. Beres-Jones, C. K. Ferreira and D. J. Reinkensmeyer, Feasibility of manual teach-and-replay and continuous impedance shaping for robotic locomotor training following spinal cord injury, *IEEE Trans. Biomed. Eng.*, vol.55, pp.322-334, 2007.

[6] Y. Su, D. Sun, L. Ren and J. K. Mills, Integration of saturated PI synchronous control and PD feedback for control of parallel manipulators, *IEEE Trans. Robot.*, vol.22, pp.202-207, 2006.

[7] Z. Taha, A. P. A. Majeed, A. F. Z. Abidin, M. A. H. Ali, I. M. Khairuddin, A. Deboucha and M. Y. W. P. Tze, A hybrid active force control of a lower limb exoskeleton for gait rehabilitation, *Biomed. Tech. Eng.*, vol.63, pp.491-500, 2018.

[8] J. A. Saglia, N. G. Tsagarakis, J. S. Dai and D. G. Caldwell, Control strategies for patient-assisted training using the ankle rehabilitation robot (ARBOT), *IEEE/ASME Trans. Mechatronics*, vol.18, no.6, pp.1799-1808, DOI: 10.1109/TMECH.2012.2214228, 2013.

[9] R. Lu, Z. Li, C. Y. Su and A. Xue, Development and learning control of a human limb with a rehabilitation exoskeleton, *IEEE Trans. Industrial Electronics*, vol.61, no.7, pp.3776-3785, DOI: 10.1109/TIE.2013.2275903, 2014.

[10] P. K. Jamwal, S. Q. Xie, S. Hussain and J. G. Parsons, An adaptive wearable parallel robot for the treatment of ankle injuries, *IEEE/ASME Trans. Mechatronics*, vol.19, no.1, pp.64-75, DOI: 10.1109/TMECH.2012.2219065, 2012.

[11] H. Kazerooni, J. L. Racine, L. Huang and R. Steger, On the control of the Berkeley lower extremity exoskeleton (BLEEX), *Proc. of the 2005 IEEE International Conference on Robotics and Automation*, Barcelona, Spain, pp.4353-4360, 2005.

[12] Z. A. Waheed and A. J. Humaidi, Design of optimal sliding mode control of elbow wearable exoskeleton system based on whale optimization algorithm, *Journal Européen des Systèmes Automatisés*, vol.55, no.4, pp.459-466, 2022.

[13] Z. Yang, Y. Zhu, X. Yang and Y. Zhang, Impedance control of exoskeleton suit based on adaptive RBF neural network, *Proceedings of the 2009 International Conference on Intelligent Human-Machine Systems and Cybernetics*, Hangzhou, China, vol.1, pp.182-187, 2009.

[14] N. A. Alawad, A. J. Humaidi and A. S. Alaraj, Observer sliding mode control design for lower exoskeleton system: Rehabilitation case, *Journal of Robotics and Control (JRC)*, vol.3, no.4, DOI: 10.18196/jrc.v3i4.15239, 2022.

[15] J. Han, From PID to active disturbance rejection control, *IEEE Trans. Industrial Electronics*, vol.56, no.3, pp.900-906, DOI: 10.1109/TIE.2008.2011621, 2009.

[16] Z. Zhang, Z. Yang, G. Zhou, S. Liu, D. Zhou and S. Chen, Adaptive fuzzy active-disturbance rejection control-based reconfiguration controller design for aircraft anti-skid braking system, *Actuators*, vol.10, pp.1-21, 2021.

[17] R. Li, T. Li, R. Bu, Q. Zheng and C. Chen, Active disturbance rejection with sliding mode control based course and path following for underactuated ships, *Mathematical Problems in Engineering*, DOI: 10.1155/2013/743716, 2013.

[18] T.-J. Su, S.-M. Wang, J. S.-H. Tsai, T.-Y. Tsou and V.-K. Tran, Design of fuzzy and linear active disturbance rejection control for insulin infusion in type 1 diabetic patients, *Int. J. Fuzzy Syst.*, vol.19, no.6, pp.1966-1977, DOI: 10.1007/s40815-017-0318-x, 2017.

[19] M. Ali and L. Mehennaoui, Active disturbance rejection control of a SCARA robot arm, *International Journal of u- and e-Service, Science and Technology*, vol.8, no.1, pp.435-446, 2015.

[20] R. Ginhoux, J. Gangloff, M. de Mathelin, L. Soler, M. M. A. Sanchez and J. Marescaux, Active filtering of physiological motion in robotized surgery using predictive control, *IEEE Trans. Robot.*, vol.21, pp.67-79, 2005.

[21] E. Zhu, J. Pang, N. Sun, H. Gao, Q. Sun and Z. Chen, Airship horizontal trajectory tracking control based on active disturbance rejection control (ADRC), *Nonlinear Dyn.*, vol.75, pp.725-734, 2013.

[22] E. H. Dulf, R. Both and C. I. Muresan, Active disturbance rejection controller for a separation column, *Porc. of the 2014 IEEE International Conference on Automation, Quality and Testing, Robotics*, Cluj-Napoca, Romania, pp.1-6, 2014.

[23] D. Zeng, Z. Yu, L. Xiong, Z. Fu, Z. Li, P. Zhang, B. Leng and F. Shan, HFO-LADRC lateral motion controller for autonomous road sweeper, *Sensors (Basel)*, vol.20, no.8, DOI: 10.3390/s20082274, 2020.

[24] D. Li, P. Ding and Z. Gao, Fractional active disturbance rejection control, *ISA Trans.*, vol.62, pp.109-119, 2016.

[25] J. Han, Auto-disturbances-rejection controller and its applications, *Control Decis.*, vol.13, pp.19-23, 1998.

[26] Z. Gao, Active disturbance rejection control: A paradigm shift in feedback control system design, *Proc. of the American Control Conference*, Minneapolis, MN, USA, 2006.

[27] Y. Long, Z. Du, L. Cong, W. Wang, Z. Zhang and W. Dong, Active disturbance rejection control based human gait tracking for lower extremity rehabilitation exoskeleton, *ISA Trans.*, vol.67, pp.389-397, 2017.

[28] X. Wu and Z. Li, Cooperative manipulation of wearable dual-arm exoskeletons using force communication between partners, *IEEE Trans. Ind. Electron.*, no.2, pp.1-10, 2019.

[29] D. Winter, *Biomechanics and Motor Control of Human Movement*, 4th Edition, John Wiley & Sons, Inc., 2009.

[30] G. Al Rezage and M. Tokhi, Fuzzy PID control of lower limb exoskeleton for elderly mobility, *2016 IEEE International Conference on Automation, Quality and Testing, Robotics (AQTR)*, Cluj-Napoca, Romania, pp.1-6, DOI: 10.1109/AQTR.2016.7501310, 2016.

[31] J. Craig, *Introduction to Robotics: Mechanics and Control*, Pearson Education, New York, NY, USA, 1986.

[32] N. A. Alawad, J. H. Amjad and A. S. Al-Araji, Improved active disturbance rejection control for the knee joint motion model, *Mathematical Modelling of Engineering Problems*, vol.9, no.2, pp.477-483, 2022.

[33] A. J. Humaidi, H. M. Badr and A. H. Hameed, PSO-based active disturbance rejection control for position control of magnetic levitation system, *2018 5th International Conference on Control, Decision and Information Technologies*, Greece, 2018.

[34] A. J. Humaidi, H. M. Badr and A. R. Ajil, Design of active disturbance rejection control for single-link flexible joint robot manipulator, *The 22nd International Conference on System Theory, Control and Computing*, 2018.

[35] N. A. Alawad, A. J. Humaidi and A. S. Alaraji, Fractional proportional derivative-based active disturbance rejection control of knee exoskeleton device for rehabilitation care, *Indonesian Journal of Electrical Engineering and Computer Science*, vol.28, no.3, pp.1405-1413, 2022.

[36] N. A. Alawad, A. J. Humaidi, A. S. M. Al-Obaidi and A. S. Alaraj, Active disturbance rejection control of wearable lower limb system based on reduced ESO, *Indonesian Journal of Science & Technology*, vol.7, no.2, pp.203-218, 2022.

[37] N. Ahmed, A. Humaidi and A. Sabah, Clinical trajectory control for lower knee rehabilitation using ADRC method, *Journal of Applied Research and Technology*, vol.20, no.5, pp.576-583, 2022.

[38] X. Chen, D. Li, Z. Gao and C. Wang, Tuning method for second-order active disturbance rejection control, *Proc. of the 30th Chinese Control Conference*, pp.6322-6327, 2011.

[39] Z. Gao, Scaling and parameterization based controller tuning, *Proc. of the American Control Conference*, pp.4989-4996, DOI: 10.1109/ACC.2003.1242516, 2003.

[40] A. J. Humaidi and H. M. Badr, Linear and nonlinear active disturbance rejection controllers for single-link flexible joint robot manipulator based on PSO tuner, *Journal of Engineering Science and Technology Review*, vol.11, no.3, pp.133-138, 2018.

[41] S. S. Husain, M. Q. Kadhim, A. S. M. Al-Obaidi, A. F. Hasan, A. J. Humaidi and D. N. Al-Husaeni, Design of robust control for vehicle steer-by-wire system, *Indonesian Journal of Science & Technology*, vol.8, no.2, pp.197-216, 2023.

[42] A. Humaidi and M. Hameed, Design and performance investigation of block-backstepping algorithms for ball and arc system, *Proc. of the 2017 IEEE International Conference on Power, Control, Signals and Instrumentation Engineering (ICPCSI)*, Chennai, India, pp.325-332, 2017.

[43] A. Humaidi and A. Hameed, Design and comparative study of advanced adaptive control schemes for position control of electronic throttle valve, *Information*, vol.10, no.2, pp.1-14, DOI: 10.3390/info 10020065, 2019.

[44] A. Hameed, A. Al-Dujaili, A. Humaidi and H. Hussein, Design of terminal sliding position control for electronic throttle valve system: A performance comparative study, *Int. Rev. Autom. Control*, vol.12, pp.251-260, DOI: 10.15866/ireaco.v12i5.16556, 2019.

[45] A. J. Humaidi and A. H. Hameed, PMLSM position control based on continuous projection adaptive sliding mode controller, *Systems Science and Control Engineering*, vol.6, no.3, pp.242-252, 2018.

[46] Z. A. Waheed, A. J. Humaidi, M. E. Sadiq, A. A. Al-Qassar, A. F. Hasan, A. Q. Al-Dujaili, A. R. Ajel and S. J. Abbas, Control of elbow rehabilitation system based on optimal-tuned backstepping sliding mode controller, *Journal of Engineering Science and Technology*, vol.18, no.1, pp.584-603, 2023.

[47] A. J. Humaidi, S. K. Kadhim and A. S. Gataa, Optimal adaptive magnetic suspension control of rotary impeller for artificial heart pump, *Cybernetics and Systems*, vol.53, no.1, pp.141-167, 2022.

[48] A. J. Humaidi and A. H. Hameed, Robustness enhancement of MRAC using modification techniques for speed control of three phase induction motor, *Journal of Electrical Systems*, vol.13, no.4, pp.723-741, 2017.

[49] S. M. Mahdi, N. Q. Yousif, A. A. Oglah, M. E. Sadiq, A. J. Humaidi and A. T. Azar, Adaptive synergetic motion control for wearable knee-assistive system: A rehabilitation of disabled patients, *Actuators*, vol.11, no.7, DOI: 10.3390/act11070176, 2022.

[50] A. Al-Jodah, S. J. Abbas, A. F. Hasan, A. J. Humaidi, A. S. M. Al-Obaidi, A. A. AL-Qassar and R. F. Hassan, PSO-based optimized neural network PID control approach for a four wheeled omnidirectional mobile robot, *International Review of Applied Sciences and Engineering*, vol.14, no.1, pp.58-67, 2023.